A&A 455, 379–384 (2006)
DOI: 10.1051/0004-6361:20065166

Astronomy & Astrophysics

Can a chondrule precursor survive a shock wave?

S. Sirono[1]

Earth and Environmental Sciences, Graduate School of Environmental Studies, Nagoya University, Nagoya 464-8602, Japan
e-mail: sirono@eps.nagoya-u.ac.jp

Received 9 March 2006 / Accepted 28 April 2006

ABSTRACT

In a shock-wave heating model, a chondrule is formed due to frictional heating between its precursor and gas. If the tensile stress inside the precursor derived from the gas dynamic pressure, is greater than the tensile strength of the precursor, the precursor is broken into smaller pieces. The yield (onset of plastic deformation) and breaking (onset of fracturing) strengths of the precursor when sintering is taken into account was calculated. The timescale of sintering is estimated. The model in Sirono & Greenberg (2000, Icarus 145, 230), in which a grain aggregate is assumed to comprise chains of spherical grains of uniform size was used. The critical packing fraction above which an aggregate can survive a shock wave is obtained. If the degree of sintering is low, the breaking strength of the aggregate decreases due to sintering. When sintering has sufficiently occurred, the aggregate can avoid breaking up. Sintering can proceed upstream of the shock wave before the passage of the shock wave.

Key words. meteors, meteoroids – interplanetary medium – solar system: general

1. Introduction

Chondrule formation is one of the most important unresolved problems in planetary science. Many models have been proposed such as lightning (Horanyi et al. 1995), outflow from the central star (Shu et al. 1996), planetesimal collision (Yamamoto et al. 1991), and turbulence (Cuzzi et al. 1996). Among them, shock-wave heating models have recently attracted considerable attention (Hood & Horanyi 1991, 1993; Ruzmaikina & Ip 1994; Iida et al. 2001; Miura et al. 2002; Miura & Nakamoto 2005a). In this model, a chondrule precursor is frictionally heated by gas after the passage of a shock wave front. Several models describing the source of the shock wave capable of producing chondrules have been proposed; accretion shock at the surface of the solar nebula (Ruzmaikina & Ip 1994), infalling of clumps of gas onto the nebula (Tanaka et al. 1998), bow shocks produced by planetesimals on eccentric orbits (Weidenschilling et al. 1998), spiral arms of the nebula (Boss 2002), and X-ray flares from the young Sun (Nakamoto et al. 2005). Although the source of the shock wave still remains uncertain, this model satisfies many constraints such as heating timescale (Miura et al. 2002), cooling timescale (Miura & Nakamoto 2005a), duration of peak temperature (Iida et al. 2001), and size distribution of chondrules (Miura & Nakamoto 2005a).

It is highly possible that the precursor of a chondrule is an aggregate of $\sim$1 μm sized grains, carried from an interstellar cloud (Greenberg 1982; Li & Greenberg 1997). Thus, we can raise a simple question: "Can a chondrule precursor survive the gas dynamic pressure after a passage of the shock wave front?" The range of the gas dynamic pressure relevant to chondrule formation is 1–1000 Pa (calculated from input parameters in Miura & Nakamoto 2005a). If the tensile strength of a precursor (grain aggregate) is weaker than the tensile stress produced by the gas dynamic pressure, the precursor might break into smaller pieces. A small precursor (less than $\sim$10 μm; Miura & Nakamoto 2005a) evaporates rapidly due to gas drag heating and does not form a chondrule. Further, the breakup of precursors affects the observed size distributions of the chondrules (Hughes 1978a,b).

Blum & Schräpler (2004) experimentally measured the tensile strength of an aggregate composed of 0.76 μm radius SiO_2 grains to be $\sim$1000 Pa. The measurements suggested that such an aggregate could probably survive a shock wave. However, an aggregate formed in the solar nebula is probably highly porous. The fractal dimension of experimentally formed aggregates is 1.4 (Krause & Blum 2004), and that of numerically generated ones is $\simeq$2 (cluster-cluster aggregation simulation; Weidenschilling & Cuzzi 1993). The mean packing fraction (volume fraction occupied by grains) of a fractal aggregate with a radius of 1 mm is $(1\ \mathrm{mm}/0.1\ \mu\mathrm{m})^{D_\mathrm{f}-3} = 10^{-4}$ (fractal dimension $D_\mathrm{f} = 2$ is adopted). This is compared to the packing fraction of the sample employed Blum & Schräpler (2004) of 0.2 whose tensile strength was $\sim$1000 Pa. The tensile strength of highly porous aggregates should be considerably less than that of a highly packed aggregate. If the packing fraction of an aggregate is low, its basic structure is a chain of grains. In this study, strengths required for splitting and bending chain, which determine the strength of an aggregate, are calculated.

It has been shown that the temperature of a precursor upstream of a shock wave front is high because of the radiation emitted by the heated precursors downstream of the wave (Desch & Connolly 2002; Ciesla & Hood 2002). Under high temperature conditions, sintering can significantly modify the strength of an aggregate (Sirono 1999). Another aim of this study is to determine the effect of sintering on the strength of the aggregate.

In the next section, the critical forces required for splitting and bending the chain are derived. The yield and breaking strengths of the aggregate are calculated based on the critical force of the chain. Further, the critical force of the chain after sintering is calculated. The timescale for sintering, which occurs at high temperatures is estimated in Sect. 3. Section 4 discusses the assumptions employed in this study. Section 5 summarizes of this study.

2. Strength of a grain chain

2.1. Before sintering

The basic unit of an aggregate is a chain of grains when the packing fraction of the aggregate is extremely low. Here, the model in Sirono & Greenberg (2000) is adopted as the structure of the grain chain. In this model, the grains are triangularly connected with an end-to-end distance l and height $l/2$. A chain comprises N grains of radius R. The number of grains N in the chain can be expressed as

$$N = \left[\left(\frac{l}{2R} - 1\right)^2 + \left(\frac{l}{2R}\right)^2\right]^{1/2} + 1. \quad (1)$$

Suppose that a grain aggregate passes through a shock wave front, and it is exposed to a headwind. Then, the forces due to the gas dynamic pressure are transmitted to the chains. If the force is small, the chain responds elastically. However, if the force is sufficiently large, the chain deforms plastically. At low temperatures, a micron-sized grain can smoothly roll around an adjacent grain without breaking (Heim et al. 1999). As a result, yielding (the onset of plastic deformation) occurs, which is caused due to the rolling of grains. The critical force for rolling $F_{\rm roll,nosint}$ (the minimum force applied at the center of a grain to start rolling) is given by (Dominik & Tielens 1997)

$$F_{\rm roll,nosint} = 6\pi\gamma\xi, \quad (2)$$

where γ is the surface energy of the grains and ξ is the critical rolling displacement of the grain, whose experimentally measured value is of the order of ten interatomic distances (Heim et al. 1999).

Suppose we fix one end of the grain chain and apply a force at the other end in the direction of the fixed end. In this case, the critical force $Y_{\rm chain,nosint}$ required for bending the triangular grain chain is given by (Sirono & Greenberg 2000)

$$Y_{\rm chain,nosint} = \frac{2F_{\rm roll,nosint}R(N+1)}{(N-3)(l/2-R)}, \quad (3)$$

where $F_{\rm roll,nosint}$ is given by Eq. (2). The yield strength of an aggregate is determined by the yielding force of the chain $Y_{\rm chain,nosint}$ due to rolling when the packing fraction of the aggregate is low ($\psi < 0.3$: Sirono & Greenberg 2000). For high packing fraction aggregates, the chain deforms due to sliding because of the lack of free space (voids) required for the rolling.

In general, the direction of the force applied to the chain is random because the direction of the chain with respect to the external force is random. However, the variation of $Y_{\rm chain,nosint}$ is not significant (a factor of two for the triangular chain assumed in this study).

The direction of the force can result in both stretching and shortening of the chain. If a stretching force is applied, the chain lengthens as a result of rolling of the grains. A further application of the force in the stretching direction results in the splitting of the chain. The critical force at which splitting occurs is (Johnson 1985, p. 127)

$$T_{\rm chain,nosint} = \frac{3\pi\gamma R}{2}. \quad (4)$$

The breaking strength of the aggregate (onset of fracturing) is determined from this splitting force. This breakage can occur due to tensile and shear deformations. Compaction does not result in the breakage of the chain. The ratio of the two critical forces (Eqs. (3) and (4)) is

$$Y_{\rm chain,nosint}/T_{\rm chain,nosint} = \frac{8\xi(N+1)}{(N-3)(l/2-R)} \ll 1, \quad (5)$$

which clearly indicates that yielding due to rolling proceeds prior to the tensile splitting of a chain. Further, Eq. (5) suggests that the compressive yield strength of the grain aggregate is less than its tensile strength. This is unusual because the compressive yield strength of normal solid materials is greater than their tensile strength, however, it is in accordance with recent experimental results obtained by Langkowski and Blum (in preparation) for low packing fraction aggregates ($\psi < 0.15$).

Each grain chain supports the stress applied to a sectional area l^2 in the aggregate. Then the breaking strength of the aggregate is given by

$$T_{\rm agg,nosint} = \frac{T_{\rm chain,nosint}}{l^2} = \frac{3\pi\gamma R}{2l^2}. \quad (6)$$

By using Eq. (3), the yield strength $Y_{\rm agg,nosint}$ of the aggregate is

$$Y_{\rm agg,nosint} = \frac{Y_{\rm chain,nosint}}{l^2} = \frac{12\pi\gamma\xi R(N+1)}{l^2(l/2-R)(N-3)} \qquad (\psi < 0.3). \quad (7)$$

When the packing fraction is high, the yield strength $Y_{\rm agg,nosint}$ of the aggregate is determined from the critical sliding force between grains and is given by (Sirono & Greenberg 2000)

$$Y_{\rm agg,nosint} = \frac{Ga_{\rm c}^2}{4l^2}\left[1 + \left(\frac{l}{l-2R}\right)^2\right]^{1/2} \qquad (\psi > 0.3), \quad (8)$$

where G is the shear modulus and $a_{\rm c}$ is the contact radius of adjacent grains.

In Sirono & Greenberg (2000), the triangular chains are periodically connected resulting in the formation of a cubic lattice. The packing fraction ψ of the aggregate for this lattice is given by

$$\psi = \frac{4\pi R^3(3N-5)}{3l^3}. \quad (9)$$

$T_{\rm agg,nosint}$ and $Y_{\rm agg,nosint}$ can be expressed as a function of ψ by using Eqs. (1) and (9) and shown in Fig. 1. We use $R = 0.76\,\mu$m, $\gamma = 0.014\ {\rm J\,m^{-2}}$, $\xi = 3.2 \times 10^{-9}$ m (Heim et al. 1999), and the shear modulus of glass $G = 22$ GPa (Johnson 1985, p. 110). The contact radius $a_{\rm c}$ is obtained from $a_{\rm c} = (9\gamma R^2(1-\nu^2)/8E)^{1/3} = 5.4 \times 10^{-9}$ m, where the Young's modulus of glass $E = 55$ GPa and the Poisson's ratio $\nu = 0.25$ (Johnson 1985, p. 110) is used. Note that $Y_{\rm agg,nosint} \ll T_{\rm agg,nosint}$ for $\psi < 0.3$, and that $Y_{\rm agg,nosint} \gg T_{\rm agg,nosint}$ for $\psi > 0.3$.

It should be noted that the yield and breaking strengths of an aggregate depend on the direction of stress. For example, the tensile strength (breaking strength with regard to tensile stress) is significantly less than the compressive strength in normal solid materials due to the presence of cracks. Therefore, the yield and breaking strengths derived above should depend on the stress tensor. The strengths exhibit a complex dependence on the arrangement of grains; the determination of this dependence is beyond the scope of this study.

On passing through a shock wave, an aggregate is exposed to a headwind. The headwind decelerates the motion of the aggregate relative to the gas, and a stress field develops inside the aggregate. Figure 2 shows the stress distribution inside an elastic sphere that experiences a headwind from the normalized dynamic pressure $P/K = 10^{-5}$, where K is the bulk modulus of

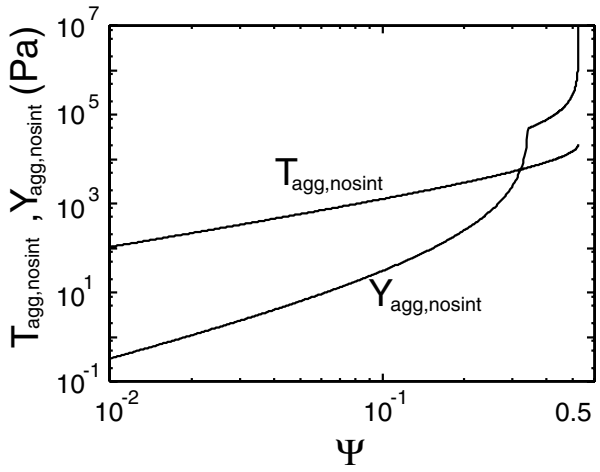

Fig. 1. The breaking strength before sintering $T_{\rm agg,nosint}$ (upper solid curve) and the yield strength before sintering $Y_{\rm agg,nosint}$ (lower solid curve) as a function of the packing fraction ψ.

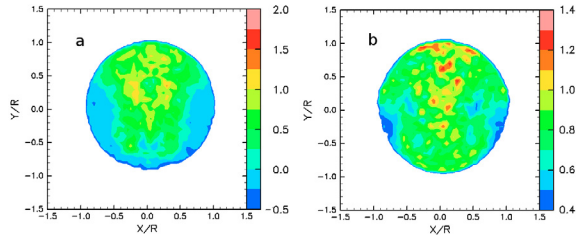

Fig. 2. The stress distribution inside an elastic sphere that experiences a gas dynamic pressure from top to bottom. **a)** the diagonal section of the stress tensor $\sigma_{ii}/3$. Tensile stress appears at the rear side. **b)** the square of the second invariant of deviatoric stress tensor $\sqrt{J_2} = \sqrt{S_{ij}S_{ij}}$, where $S_{ij} = \sigma_{ij} - \sigma_{kk}\delta_{ij}/3$. The stress values in the figure are normalized with respect to the applied gas dynamic pressure.

the aggregate. The ratio indicates that the deformation is purely elastic. The bulk modulus can be calculated as (using Eqs. (17) and (20) in Sirono & Greenberg 2000) $K = 0.33$ Pa for $\psi = 10^{-3}$, 42 Pa for 10^{-2}, 1.1×10^4 Pa for 0.1. The shear modulus is set to $K/2$, and radius = 1 mm. The wind blows from top to bottom in Fig. 2. I used a smoothed particle hydrodynamics (SPH) code (Sirono 2004) with 53117 SPH particles was used. Figure 2a indicates the diagonal section of the stress tensor $\sigma_{ii}/3$ (compression is positive), and b indicates the square of the second invariant of the deviatoric stress tensor $\sqrt{J_2} = \sqrt{S_{ij}S_{ij}}$, where $S_{ij} = \sigma_{ij} - \sigma_{kk}\delta_{ij}/3$; this represents the measure of the shear stress.

Figure 2a clearly shows that both compressive and tensile stresses appear inside the aggregate. The maximum tensile stress is $0.5P$. Therefore, if $T_{\rm agg,nosint} > P$, a spherical aggregate can safely survive a shock wave. On the other hand, if $T_{\rm agg,nosint} < 0.5P$, of the aggregate begins to partial break at its rear side. Furthermore, in the region of compressive stress, compaction proceeds when $Y_{\rm agg,nosint} < P$. Shear deformation also proceeds in a substantial section of the aggregate when $Y_{\rm agg,nosint} < P$ (see Fig. 2b).

The maximum tensile stress depends on the shape of the aggregate; therefore, the factor of 0.5 varies according to the shape.

The critical packing fraction above which the aggregate survives ($T_{\rm agg,nosint} > P$) can be estimated using Fig. 1. The critical packing fraction ψ is 0.01 for $P = 100$ Pa; and 0.08 for $P = 1000$ Pa. A packing fraction below these values results in a partial breakup of the aggregate.

2.2. After sintering

Two adjacent grains are connected by a neck. The neck radius without sintering is determined from the balance between surface adhesion and elastic repulsion of the grain. The surface adhesion is due to van der Waals attraction, which is significantly weaker than the covalent bonding of Si-O. In fact, a small surface energy 0.014 J m^{-2} is observed (Heim et al. 1999) for SiO_2 grains without sintering as compared to the theoretical value (0.58 J m^{-2}) for the 110 plane of β cristobalite (Bruce 1966). A grain can roll around an adjacent grain, as shown experimentally (Heim et al. 1999). The balance between surface adhesion and elastic repulsion enables smooth rolling.

As sintering proceeds, molecules flow to the neck. Evidently, no elastic stress is present in the increased region of the neck. Furthermore, the molecules in the neck reorganize, and form covalent bonds between the molecules at the surfaces of the grains in contact, instead of forming the weak van der Waals bonding. In this case, the grain cannot roll around an adjacent grain without breaking the contact.

When we apply a bending moment $F_{\rm roll,sint}R$ at the center of a grain while the adjacent grain is fixed, a tensile stress $\sigma_{zz} = F_{\rm roll,sint}R/W$ is developed at the edge of the neck with radius αR, where $W = \pi(\alpha R)^3/4$ is the section modulus. If the stress σ_{zz} attains the value of the yield strength of the material $Y_{\rm mat}$, the contact starts to break. This condition yields to the critical rolling force $F_{\rm roll,sint}$ after sintering given by

$$F_{\rm roll,sint} = \frac{\pi\alpha^3 R^2 Y_{\rm mat}}{4}. \tag{10}$$

There are two possibilities when the sintered contact breaks: (1) no new contact is formed and the chain breaks into two pieces; and (2) a new van der Waals contact is formed between nearby chains or between the two separated pieces of the chain. In case (2), the tensile strength of the chain attains the value it had before sintering. In case (1), the number of chains carrying the applied stress decreases, and the tensile strength of the aggregate also decreases.

After sintering, the critical force required to plastically bend a chain $Y_{\rm chain,sint}$ is obtained by Eq. (3) with Eq. (10) rather than Eq. (2). Recall that rolling leads to the breaking of a contact, which is in contrast with the non-sintered case. Therefore, $Y_{\rm chain,sint}$ is the critical force at which a chain breaks as a result of bending. The critical force for splitting a chain after sintering is $T_{\rm chain,sint} = \pi(\alpha R)^2 Y_{\rm mat}$. The ratio of the bending strength of a chain $Y_{\rm chain,sint}$ to the splitting strength after sintering $T_{\rm chain,sint}$ is

$$Y_{\rm chain,sint}/T_{\rm chain,sint} = \frac{\alpha R(N+1)}{4(N-3)(l/2-R)} \ll 1. \tag{11}$$

This equation clearly shows that breaking due to bending is more likely to proceed instead of splitting. As a result, $Y_{\rm chain,sint}$ determines the breaking strength of the aggregate after sintering $T_{\rm agg,sint}$, which can be written as

$$T_{\rm agg,sint} = \frac{Y_{\rm chain,sint}}{l^2} = \frac{\pi\alpha^3 R^3 Y_{\rm mat}(N+1)}{2l^2(l/2-R)(N-3)}. \tag{12}$$

The four non-solid lines in Fig. 3 indicate $T_{\rm agg,sint} = P$; above this value, an aggregate can survive passing through a shock wave with a gas dynamic pressure P. A large degree of sintering α or packing fraction ψ is necessary to avoid partial breaking. The input parameters are the same as those used in Fig. 1. In this study, $Y_{\rm mat} = 7.3 \times 10^8$ Pa (calculated from an empirical formula for

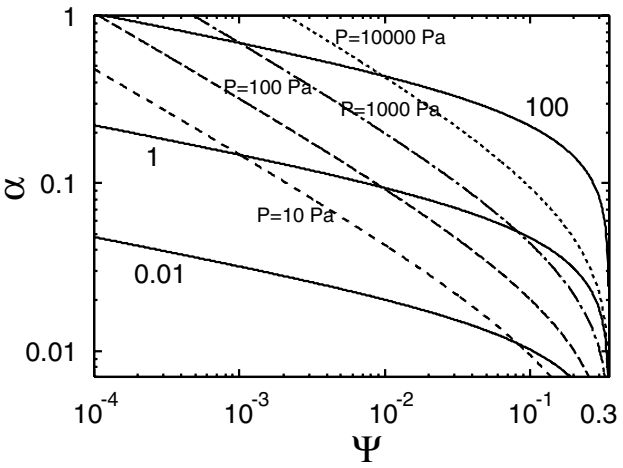

Fig. 3. The relation between critical packing fraction and α (Eq. (12)) above which an aggregate can survive a shock wave (three non-solid lines). From right to left, the gas dynamic pressure P is 10 000, 1000, 100, and 10 Pa. The contour lines of the ratio $Y_{\rm chain,sint}/T_{\rm chain,nosint}$ (three solid lines). Below $Y_{\rm chain,sint}/T_{\rm chain,nosint} = 1$, the breaking strength of the aggregate decreases as a result of sintering.

ideal yield strength of solids $G/30$, Kittel 2004; with the shear modulus of glass $G = 22$ GPa, Johnson 1985, p. 110) is selected. An ideal material strength is adopted because the radius of the chain should be micron sized and the number of cracks should be small. The value of α before sintering can be calculated as $\alpha = a_{\rm c}/R = 7.1 \times 10^{-3}$. As ψ approaches to 0.3, the breaking strength due to rolling substantially increases (Eq. (12)), and the critical α required for the survival falls below the initial $\alpha = 7 \times 10^{-3}$ even for the shock pressure of 10^4 Pa.

If the gas dynamic pressure P is greater than the breaking strength $T_{\rm agg,sint}$, chains inside the aggregate start to break due to bending. As the aggregate deforms, the sintered contacts break and new van der Waals contacts are formed. Therefore, the strength of a sintered aggregate can significantly change as a result of deformation. The three solid lines in Fig. 3 denote the contour lines of $Y_{\rm chain,sint}/T_{\rm chain,nosint}$ the ratio of the breaking strength of a chain after sintering to that before sintering. Suppose that the sintered aggregate, with values of α and ψ such that $Y_{\rm chain,sint}/T_{\rm chain,nosint} = 100$, starts to deform. As the deformation of the aggregate proceeds, new van der Waals contacts between these chains are formed. The strength of the newly formed contact is $T_{\rm chain,nosint}$. The breaking strength after deformation depends on the number of the newly formed contacts. The tensile strength of the deformed aggregate is reduced to 0.01 times of that before sintering for $Y_{\rm chain,sint}/T_{\rm chain,nosint} = 100$; this occurs when the number of broken sintered contacts and newly formed contacts are the same.

Below the line that indicates $Y_{\rm chain,sint}/T_{\rm chain,nosint} = 1$, the tensile strength of the aggregate *decreases* due to sintering, because a contact can break due to bending of the chain. A small degree of sintering can reduce the breaking strength of the aggregate by a factor of 100. For example, consider an aggregate with a packing fraction of 10^{-2}. The breaking strength before sintering is 100 Pa (see Fig. 1). If sintering proceeds such that $\alpha = 0.02$, the contact area increases by a factor of $(0.02/0.007)^2 = 8$ and $Y_{\rm chain,sint}/T_{\rm chain,nosint} = 0.01$. There is no elastic stress inside the newly formed area, which leads to the breaking of the contact due to bending. After sintering, the breaking strength becomes 0.1 Pa. Hence, the small degree of sintering promotes the partial breaking of the aggregate.

3. Sintering timescale of an aggregate

After the passage of a shock wave front, the aggregate is heated due to gas friction. A highly heated aggregate emits thermal radiation. The radiation field in the region of chondrule formation is sufficiently strong to heat the aggregates upstream of the shock wave front (Desch & Connolly 2002; Ciesla & Hood 2002), where the aggregate moves with the gas and frictional heating has not yet started.

Miura & Nakamoto (2005b) performed a detailed simulation of the radiative transfer on both sides of a shock wave front. Assuming a planar shock wave front, they calculated the temperature evolution of precursors. They included non-equilibrium chemical reactions of 32 gas species, and radiative heating due to line emissions in addition to continuum emission. The number density of molecules was 10^{20} m^{-3}, and the gas velocity was 10 km s^{-1}. The peak temperature of the precursors upstream of the wave depends on the total optical depth τ upstream of the wave, and the temperature varies as follows: 1210 K for $\tau = 0.73$, 1300 K for $\tau = 2.45$, and 1440 K for $\tau = 4.89$. The time for which the temperature increases is ∼1 h. Desch & Connolly (2002) calculated the temperature evolutions of precursors including the dissociation of hydrogen molecules. In their standard case (gas density of 10^{-9} g cm^{-3} and velocity of 7 km s^{-1}), the temperature of a precursor is maintained greater than 1500 K for 64 min. A low temperature (1120 K) and long duration (100 h) is reported for the shock wave front in gas with a density of 10^{-9} g cm^{-3} and velocity of 8.5 km s^{-1} (Ciesla & Hood 2002). In this case, a solar solids-to-gas ratio of 0.003 is used. When this ratio increases, the duration reduces (3.5 h for a ratio of 0.09).

Sintering results in a molecular flow to the neck connecting adjacent grains. Poppe (2003) conducted sintering experiments of aggregates comprising 0.78 μm radius SiO_2 grains. He measured the radii of necks $x(t)$ as a function of the heating time and found that the data adequately fit the following formula (Nichols & Mullins 1965)

$$x(t) = \left(\frac{25R^2 d\gamma_{\rm s}\Omega D(T)}{kT} t \right)^{1/6}, \tag{13}$$

where Ω denotes the molecular volume; d the molecular diameter; k Boltzmann's constant; T the temperature; $\gamma_{\rm s}$ the surface energy for diffusive sintering; and $D(T)$ the surface diffusion constant. The temperature-dependent surface diffusion constant $D(T)$ is given by

$$D(T) = c_1 \exp(-c_2/T). \tag{14}$$

Poppe (2003) experimentally determined the following values: $c_1 = 5.53 \times 10^{11}$ m^2 s^{-1} and $c_2 = 77420$ K. The sintering timescale of the aggregate comprising 0.76 μm radius SiO_2 grains can be obtained by substituting $\Omega = 4.98 \times 10^{-29}$ m^{-3}, $d = 4.56 \times 10^{-10}$ m, and $\gamma_{\rm s} = 0.3$ J m^{-2} (Poppe 2003). Further, the time $t_{\rm sint}(\alpha, T)$ required for the neck radius to grow to $x = \alpha R$ is given by

$$\begin{aligned} t_{\rm sint}(\alpha, T) &= \alpha^6 \frac{kR^4 T \exp(c_2/T)}{25 d\gamma_{\rm s}\Omega c_1} \\ &= 2.8 \times 10^{-23} T \exp(77420/T)\alpha^6 \,{\rm s}, \end{aligned} \tag{15}$$

where T is expressed in Kelvin.

Here we calculate two timescales of sintering. One is $t_{\rm sint}(1, T)$, which corresponds to a perfect neck. According to

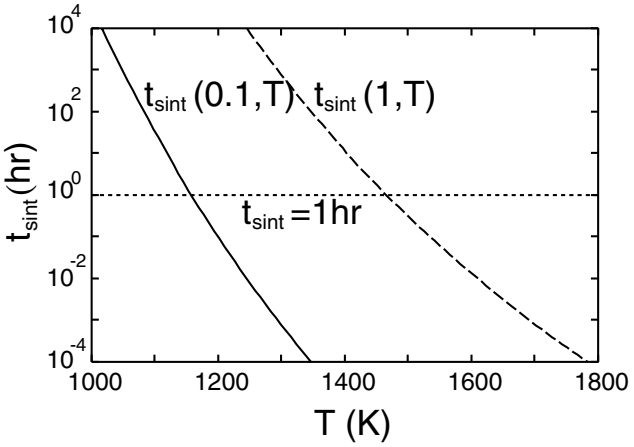

Fig. 4. Timescales $t_{\rm sint}(\alpha, T)$ with regard to sintering as a function of temperature T and the neck radius α normalized with grain radius R. Timescales with regard to a substantial increase in the contact area $t_{\rm sint}(0.1, T)$ (solid curve) and with regard to shrinkage $t_{\rm sint}(1, T)$ (dashed curve) are shown. The horizontal dotted line represents a time of 1 h.

Fig. 3, the strength of the sintered aggregate with $\alpha = 1$ exceeds 1000 Pa when $\psi > 10^{-3}$. Poppe (2003) showed that an aggregate begins shrinking and the radius of each grain increases when $\alpha > 0.9$ (sample f in Poppe 2003). This shrinkage results in the growth of the necks beyond the initial grain size, and new contacts are formed. Therefore, even if ψ is low, the structure of the aggregate changes and the strength drastically increases with α. Therefore, $t_{\rm sint}(1, T)$ represents the timescale for a structural change in order to avoid the aggregate from breaking up.

The other timescale is $t_{\rm sint}(0.1, T)$. When the value of α increases to 0.1, the breaking strength of the aggregate after sintering is close to that before sintering (see Fig. 3). Below $\alpha = 0.1$ the breaking strength decreases due to sintering.

Figure 4 shows the two timescales in the relevant temperature range. It can be observed that the timescale for shrinkage is less than 1 h above $T = 1450$ K. Therefore, the breakup of an aggregate can be avoided when the temperature is greater than $T = 1450$ K. A substantial increase in the strength due to sintering is expected in the range $1150 < T < 1450$ K. Below 1150 K, the breaking strength of the aggregate is reduced and the probability of breaking increases.

Many mechanisms to produce a shock wave have been proposed. The temperature increase resulting from radiation depends on the shock forming mechanism and the shape of the shock wave. The degree of sintering is determined by the integrated molecular flux. The temperature evolution of an aggregate is necessary to calculate the value of α for each shock wave model.

An aggregate will pass through shock waves a number of times. In each of these events, sintering occurs to some extent depending on the strength of the radiation and gas frictional heating. The strengths of the aggregates change as they pass through a shock wave. The survival of the aggregate depends on the value of α when the gas dynamic pressure increases.

4. Discussion: examination of assumptions

There are two essential assumptions in the model of a grain aggregate. One is the homogeneity of the internal structure of the aggregate. With regard to the model adopted in this study, identical grain chains are periodically connected, resulting in the formation of an aggregate. In fact, the length, shape, and connectivity of the chain vary. Long chains play a crucial role in determining the strength of an aggregate; because they are comparatively weak (see Eq. (5)). If there is a variation in the chain length, it is possible that the aggregate contains longer chains instead of a uniform length assumed in this study. Then, based on this viewpoint, Eqs. (6) and (7) might overestimate the strengths.

The other crucial assumption is that the chain is singly-connected. Every grain in a chain has two contacts, except the junction grains that connect to adjacent chains. If this is not the case, the bending of a chain may involve the splitting of a contact. This effect should be important for aggregates with a high packing fraction.

It is difficult to clarify these effects quantitatively, because these quantities depend on the formation history of the aggregate. Here, a comparison between the calculated values and experimental data in Blum & Schräpler (2004) is drawn. Equation (6) gives a breaking strength of 3000 Pa at $\psi = 0.2$ as compared to the experimentally measured mean value of 1000 Pa. This difference can be attributed to the existence of long chains (large voids) that reduce the tensile strength. On the other hand, Eq. (7) gives the compressive yield strength at $\psi = 0.2$ as 260 Pa as compared to the value of 1300 Pa in Blum & Schräpler (2004). This difference is probably due to multiple contacts in the grain chain, which can be observed in their scanning electron microscope images.

Spherical grains have been assumed in this study. If the surface of the grain is rough, multiple contacts are possible between the grains. A stable configuration requires three contacts. Multiple contacts increase the critical rolling force, because the splitting of a contact is necessary in order to roll a grain. As a result, the critical packing fraction required for compaction to occur (Fig. 3) increases.

The sintering of SiO_2 grains has been discussed. The grains may comprise two different compounds other than silicates; ices and organics (Greenberg 1982). The temperature dependent diffusion constant (Eq. (14)) significantly depends on the activation energy E. The activation energies for ices and organics are less than those for silicates; sintering proceeds at lower temperatures for these materials. These materials evaporate completely in chondrule forming shock waves. However, the collisional evolution of aggregates containing these materials essentially depends on sintering because sintering significantly modifies the strengths of the grain aggregates, as shown in this study and by Sirono (1999).

5. Summary

In this study, the bending and splitting strengths of a grain chain are derived. The yield and breaking strengths of an aggregate are determined by the bending and splitting strengths of the grain chain, respectively. The critical packing fraction above which the aggregate can survive is calculated. With regard to the non-sintered case, it is found that compaction proceeds in a substantial part of the aggregate where the compressive stress dominates.

It is shown that sintering can significantly modify the strength of a grain chain. As sintering proceeds, an aggregate breaks as a result of the bending of the chain because the stress inside the neck connecting adjacent grains relaxes. If the degree of sintering is low, the tensile strength of the aggregate decreases because the chain breaks as a result of bending after sintering. A small degree of sintering promotes partial breaking of an aggregate. There exists a threshold degree of sintering above

which the tensile strength of the aggregate increases due to sintering.

Further, the timescale of sintering is estimated. If the temperature of the aggregate is high ($T > 1450$ K for 0.76 μm SiO_2 grains, Poppe 2003), sintering proceeds up to the stage at which the aggregate shrinks. Such an aggregate can survive a shock wave due to an increase in its strength. In the intermediate temperature range ($1150 < T < 1450$ K), the tensile strength of the aggregate increases due to sintering. If the temperature of the aggregate is low ($T < 1150$ K), sintering proceeds only to small amount. In this case, the breaking strength of the aggregate decreases. The probability of the breaking of such an aggregate increases due to sintering.

Acknowledgements. The author greatly thanks to J. Blum, T. Poppe and S. J. Weidenschilling, who provided critical and constructive comments. This research was partially supported by the Ministry of Education, Science, Sports and Culture, Grant-in-Aid for Young Scientists (B), No. 18740273, 2006.

References

Blum, J., & Schräpler, R. 2004, Phys. Rev. Lett., 93, 115503
Boss, A. P. 2002, ApJ, 576, 462
Bruce, R. H. 1966, Sci. Ceramics, 2, 359
Ciesla, F. J., & Hood, L. L. 2002, Icarus, 158, 281
Desch, S. J., & Connolly, H. C., Jr. 2002, Meteorit. Planet. Sci., 37, 183
Heim, L.-O., Blum, J., Preuss, M., & Butt, H.-J. 1999, Phys. Rev. Lett., 83, 3328
Hood, L. L., & Horanyi, M. 1991, Icarus, 93, 259
Hood, L. L., & Horanyi, M. 1993, Icarus, 106, 179
Horanyi, M., Morfill, G., Goertz, C. K., & Levy, E. H. 1995, Icarus, 114, 174
Kittel, C. 2004, Introduction to solid state physics, 8th ed. (New York: John Wiley and Sons)
Krause, M., & Blum, J. 2004, Phys. Rev. Lett., 93, 021103
Greenberg, J. M. 1982, in Comets, ed. L. L. Wilkening (Tucson: Univ. of Arizona Press), 131
Hughes, D. W. 1978a, Earth Planet. Sci. Lett., 38, 391
Hughes, D. W. 1978b, Earth Planet. Sci. Lett., 39, 371
Iida, A., Nakamoto, T., Susa, H., & Nakagawa, Y. 2001, Icarus, 153, 430
Johnson, K. L. 1985, Contact mechanics. (Cambridge: Cambridge Univ. Press)
Li, A., & Greenberg, J. M. 1997, A&A, 323, 566
Miura, H., & Nakamoto, T. 2005a, Icarus, 175, 289
Miura, H., & Nakamoto, T. 2005b, Antarctic Meteorite Research, 18, 239
Miura, H., Nakamoto, T., & Susa, H. 2002, Icarus, 160, 258
Nakamoto, T., Hayashi, M. R., Kita, N. T., & Tachibana, S. 2005, in Proceedings of Chondrites and the Protoplanetary Disk 2004, 883
Nichols, F. A., & Mullins, W. W. 1965, J. Appl. Phys., 36, 1826
Poppe, T. 2003, Icarus, 164, 139
Ruzmaikina, T. V., & Ip, W. H. 1994, Icarus, 112, 430
Shu, F. H., Shang, H., & Lee, T. 1996, Science, 271, 1545
Sirono, S. 1999, A&A, 347, 720
Sirono, S., & Greenberg, J. M. 2000, Icarus, 145, 230
Tanaka, K. K., Tanaka, H., Nakazawa, K., & Nakagawa, Y. 1998, Icarus, 134, 137
Weidenschilling, S. J., & Cuzzi, J. N. 1993, in Protostars and Planets III, ed. E. H. Levy, & J. I. Lunine (Tuscon: Univ. Arizona Press), 1031
Weidenschilling, S. J., Marzari, F., & Hood, L. L. 1998, Science, 279, 681
Yamamoto, T., Kozasa, T., Honda, R., & Mizutani, H. 1991, in Abstracts of the Lunar and Planetary Science Conference, 22, 1533